Diagnostic Pathology

RESEARCH Open Access

ITGA5 is associated with prognosis marker and immunosuppression in head and neck squamous cell carcinoma

Jianmin Liu[1†], Yongkuan Wang[2†], Xi Chen[2], Xiaofang Chen[2] and Meng Zhang[2*]

Abstract

Background Head and neck squamous cell carcinoma (HNSCC) is a major tumor that seriously threatens the health of the head and neck or mucosal system. It is manifested as a malignant phenotype of high metastasis and invasion caused by squamous cell transformation in the tissue area. Therefore, it is necessary to search for a biomarker that can systematically correlate and reflect the prognosis of HNSCC based on the characteristics of head and neck tumors.

Methods Based on TCGA-HNSCC data, R software was used to analyze gene expression, correlation, Venn diagram, immune invasive and immunosuppressive phenotypes respectively. The intrinsic effect of ITGA5 on the malignant phenotype of HNSCC cells was verified by cell experiments. Immunohistochemical images from The Human Protein Atlas (THPA) database display the differences in the expression of related proteins in HNSCC tissues. Based on functional enrichment and correlation analysis, the prognostic value of ITGA5 for HNSCC was explored, and the expression level of ITGA5 may affect the chemotherapy of targeting the PI3K-AKT.

Results In this study, the target gene ITGA5 may be identified as a valuable prognostic marker for HNSCC. The results of enrichment analysis showed that ITGA5 was mainly involved in the dynamic process of extracellular matrix, which may affect the migration or metastasis of tumor cells. Meanwhile, ITGA5 may be closely related to the infiltration of M2 macrophages, and its secretory phenotypes TGFB1, PDGFA and PDGFB may affect the immunosuppressive phenotypes of tumor cells, which reflects the systemic influence of ITGA5 in HNSCC. In addition, the expression levels of ITGA5 were negatively correlated with the efficacy of targeting PI3K-AKT chemotherapy.

Conclusion ITGA5 can be used as a potential marker to systematically associate with prognosis of HNSCC, which may be associated with HNSCC malignant phenotype, immunosuppression and chemotherapy resistance.

Keywords HNSCC, ITGA5, Extracellular matrix, Immune infiltration, Immunosuppression, Chemotherapy resistance

† Jianmin Liu and Yongkuan Wang contributed equally to this work.

*Correspondence:
Meng Zhang
ameng0838@126.com
[1]Department of Head and Neck Surgery, Sichuan Cancer Hospital, Chengdu City, Sichuan Province, China
[2]Department of Otolaryngology/Head and Neck surgery, People's Hospital of Deyang City, Deyang City, Sichuan Province, China

Introduction

HNSCC has become the sixth most common tumor in the world, and it has become a major threat to the health of the head and neck of patients, such as there were 890,000 new cases and 450,000 deaths in 2018 [1, 2]. HNSCC belongs to a category of multi-type tumors, which mainly originate from the mucosal epithelium of the mouth, pharynx and larynx, and is the most common malignant tumor of the head and neck [3, 4]. Since the HNSCC belongs to mucosal cell carcinosis, it shows high metastasis and invasiveness, which become the focus and difficulty of clinical treatment of HNSCC [3, 5–7]. In addition, the high immune infiltration of HNSCC may be an important phenotype for maintaining tumor adaptive survival, and its myeloid derived macrophages may be a typical representative [3, 7, 8]. Particularly, M2 macrophages are regulated by IL10 and TGFB1 in the tumor microenvironment, and the secretory phenotype of this cell will affect the stemness and metastasis activity of HNSCC cells [3, 7]. The high metastasis of tumor cells from HNSCC as a typical malignant phenotype of most mucosal and squamous cell carcinomas, which has become the focus of clinical prognostic and marker research [5, 9]. Therefore, to find a more valuable biomarker about metastasis and invasiveness for tumor cells, it is necessary to systematically analyze the correlation and prognostic value between the malignant phenotype and this marker based on HNSCC.

Integrin subunit α 5 (ITGA5) is derived from a protein of the integrin α-chain family, which is important for cell adhesion and signaling processes [10–12]. Studies have shown that ITGA5 is closely related to the malignant phenotypes of tumors, such as proliferation, invasion and metastasis [11, 12]. The level of ITGA5 contributes to the progression of stemness and chemotherapy resistance of tumor cells [12, 13]. In addition, there is evidence that ITGA5 has predictive or prognosis value in breast cancer, lung cancer and pancreatic cancer cells metastasis [14, 15], reflecting that ITGA5 is closely correlated with tumor cell metastasis-related phenotypes. New evidence suggests that ITGA5 may serve as a determinant of immune infiltration and a prognostic biomarker for gastrointestinal tumors and glioma [10, 16]. In summary, ITGA5 not only affects the malignant phenotype of tumor cells, but also influences immune infiltration via tumor microenvironment [10]. Based on these characteristics, ITGA5 may serve as an important biomarker that systematically links the phenotype of malignant tumor with external and internal objective conditions.

Although there have been studies and reports on ITGA5 in HNSCC related markers [17–19]. However, the systematic effects and associations of ITGA5 in HNSCC have not been studied or reported, such as tumor cell proliferation and metastasis-related phenotypes (intrinsic effects), immune cell infiltration and immunosuppressive phenotypes (extrinsic effects). Based on the screening and prognostic evaluation, ITGA5 as a possible biomarker from we determined that ITGA5 gene is related to the dynamic regulation of tumor extracellular matrix by cell experiments and enrichment analysis. In addition, ITGA5 was closely related to TGFB1 secretion phenotype of M2 macrophages by the correlation analysis of immune infiltration. Based on these results, the correlation mechanism of ITGA-TGFB1-PDCD1LG2/CD47 may reflects that ITGA5 can systematically affect the immunosuppression phenotype and progression of HNSCC. Meanwhile, we found that ITGA5 levels were positively correlated with the activity of the AKT-mTOR pathway and significantly affected the chemotherapy efficacy of the relevant targets. In summary, ITGA5 may serve as a potential marker that systematically reflects the prognostic value of HNSCC, which further may be a potential therapeutic target.

Materials and methods

HNSCC samples

The RNA-seq transcriptome data and related clinical information were obtained from The Cancer Genome Atlas (TCGA) database (https://www.cancer.gov/ccg/research/genome-sequencing/tcga). There are 528 cases HNSCC and 44 cases adjacent samples included in this study.

Cell culture

All cells involved in this study were purchased from American Type Culture Collection (ATCC). WUS-HN30, YD-8, SNU-46 and FaDu cell lines were cultured in DMEM/MEM (Gibco) supplied with 10% fetal bovine serum (Gibco) and 1% penicillin - streptomycin (100 μg/mL) at 37 °C in a humidified incubator with 5% CO2. The digestion and passage of cells involve the use of trypsin and phosphate buffers (PBS) (Biosharp, China).

Real-time qPCR

Total RNA from cells or tissues was extracted using TRIzol reagent (Invitrogen). Quantitative PCR (qPCR) was applied using SYBR Green PCR Master Mix (Takara Bio) on a Quant Studio 3 System (Thermo Fisher, Life). Relative expression was calculated by normalization to GAPDH. The primers for ITGA5 were designed by online tool Primer Bank (https://pga.mgh.harvard.edu/primerbank/), and the primer (ITGA5, Primer Bank ID: 5623702.

8c2): Forward primer: 5' GCCTGTGGAGTACAAGTC CTT 3', Reverse primer: 5' AATTCGG.

GTGAAGTTATCTGTGG 3'; (GAPDH, Primer Bank ID: 378404907c1): Forward primer: 5' GGAGCGAGATC

CCTCCAAAAT 3', Reverse primer 5' GGCTGTTGTCA TACTTCTCATG.

G 3'.

Western blot

The 20 μg protein per sample extract from cell samples, which were separated by 12% SDS-PAGE. After transferring to a PVDF membrane and blocking with 5% skimmed milk, the primary antibodies were incubated overnight at 4℃. After incubation with secondary antibodies for 1 h at room temperature. The protein bands were visualized using enhanced chemiluminescence reagents (Millipore). The antibodies involved in this study include anti-ITGA5 (Rabbit, ab112183, Abcam), anti-GAPDH (Rabbit, ab181602, Abcam) and Goat anti-Rabbit IgG HRP (H&L) (ab6721, Abcam).

Wound healing and trans-well assay

The tumor cells were seeded into the 6-well plate. After incubation for overnight, and the cell density reached 100%. Equal wounds were made by 10 μL tips. The images of wound were obtained under a microscope (Nikon) at 100 × magnification. Migration assessed using Trans-well plate, 5×10^4 cells were resuspended in 250 μL of serum free medium in the upper chamber (8 μm pore size, Corning) while the lower chambers were filled with 750 μL of complete medium. After incubating for 24 h at incubator, the upper chambers were fixed with 100% methanol for 10 min and stained with 0.1% crystal violet at room temperature. The number of transmembrane cells was calculated under a microscope (Nikon).

Colony formation and cell counting Kit-8 (CCK-8) assay

There are 200 cells per well were seeded and incubated for 14 days. The colonies were fixed using 100% methanol for 10 min at room temperature and stained with 0.1% crystal violet for 20 min at room temperature. About 500 cells per well were seeded into 96-well plates. The viability of cells was determined using a CCK-8 assay (Bimake) everyday by measuring the absorbance at 450 nm (OD450, BioTek). The absorbance was normalized to the baseline.

Immunohistochemical (IHC)

The IHC images of HNSCC involved in this study are all from The Human Protein Atlas database (https://www.proteinatlas.org/), which contains the expression of existing related proteins and the IHC results of tumor pathological tissues (all images contain the sample number).

KEGG and GO enrichment analysis

The enrichment analyses included KEGG (Kyoto Encyclopedia of Genes and Genomes) and GO (Gene Ontology) in this study. RNA-sequencing expression (level 3) profiles and corresponding clinical information for HNSCC were downloaded from the TCGA dataset (https://portal.gdc.com). Using the limma package in the R software to study the differentially expressed mRNA. "Adjusted $P<0.05$ and Log_2FC (Fold Change)>1 or $Log_2FC<-1$" were defined as the threshold for the differential expression of mRNAs. Meanwhile, online enrichment analysis was performed using Metascape (https://metascape.org/gp/index.html#/ma.

in/step1) [20].

Gene set enrichment analyses (GSEA)

Dataset of HNSCC was downloaded from the GEO database and then GSEA (http://software.broadinstitute.org/gsea/index.jsp). The overall differential genes in this dataset were used as the data source for analysis without additional conditional screening (R v4.2.1, R Package: cluster Profiler [4.4.4]). GSEA enrichments were estimated by normalized enrichment score (NES) [21]. The significance of the results was assessed with FDR<0.25 level, $P<0.05$, and FDR<0.25 levels.

Bioinformatics analysis and drug susceptibility analysis

Gene expression differential analysis, survival prognosis analysis (K-M survival curve, R Package: survival[3.3.1], survminer[0.4.9], ggplot2[3.3.6]) [22], immune infiltration analysis (R package: GSVA[1.46.0], ggplot2[3.3.6]) [23], gene expression correlation analysis (R package: ggplot2[3.3.6]), nomogram analysis (R package: survival[3.3.1], rms[6.3-0]) [22], risk analysis (R package: survival[3.3.1], rms[6.3-0]) [22], Venn diagram (R package: ggplot2[3.3.6], VennDiagram[1.7.3]), ROC curve (Calibration curves, R package: pROC[1.18.0], ggplot2[3.3.6]) [22] in HNSCC were all implemented by R v4.0.3 software package. All the analysis results were represented by Spearman as the correlation coefficient (R), and $P<0.05$ was the significant result.

Single gene difference analysis: Based on the expression of a single molecule, the difference analysis was divided into high and low expression groups. The reference group was: Low. Based on the sequencing data of TCGA-HNSCC (504 cases), we sorted the gene expression according to TPM value, and then divided the gene expression into 252/252 cases. This process is implemented with software: R (4.2.1) version R package: DESeq2[1.36.0], edgeR[3.38.2].

The correlation analysis and drug susceptibility analysis involved in this study were completed by R software v4.0.3, R package: pRRophetic and based on TCGA database, and the results were represented as Spearman correlation. in addition, Drug susceptibility analysis was performed by combining TCGA-HNSCC sample data with the Genomics of Drug Sensitivity in Cancer (GDSC) database [24, 25].

Statistical analysis

Statistical analyses were performed by SPSS version 16.0 and GraphPad Prism v8.0. The results of data are displayed as the Mean ± SD. Student's t - test was applied to determine the difference in data. All experiments were repeated at least three times. *P < 0.05, **P < 0.01, ***P < 0.001.

Results

Identification of target genes ITGA5

In general, genes upregulated in tumors are positively correlated with risk genes, and there are common characteristics between them. Therefore, 1624 up-regulated genes (Fold change, FC > 2, P < 0.05) and 1537 risk genes (Hazard ratio, HR > 1, P < 0.05) from TCGA-HNSCC were analyzed by Venn Diagram, which obtained 242 genes in common (Fig. 1A). We performed KEGG and GO enrichment analyses, and the results of the top 20 (- Log_{10}(P) > 5) indicate that these genes may be involved in the organization and regulation of the extracellular matrix, with related entries also including cell adhesion and behavior (Fig. 1B, where the red arrow is pointing, based on the most significant features of the enrichment Top 2 enrichment pathways, the similar pathways are further labeled). This result is consistent with the enrichment analysis of differential genes from TCGA-HNSCC (Supplementary Fig. 1A, B, where the red arrow is pointing). These results suggest that the up-regulated risk gene populations in HNSCC may be mainly involved in tumor extracellular matrix and related biological processes.

To further screen out the target genes, we conducted Venn diagram analysis of the genes involved in the above four items (Fig. 1B, where the red arrow is pointing), and the results showed that there were three genes that belonged to their common parts, which are FN1, ITGA5 and ABL2 (Fig. 1C). The expression difference of these genes for HNSCC reflects that ITGA5 is more significant than FN1 and ABL2 (Fig. 1D, E, ***P < 0.05. Unpaired samples: Normal: 44 cases, Tumor: 504 cases. Paired samples: Normal: 44 cases, Tumor: 44 cases) In addition, the difference between the high and low expression groups of ITGA5 in patients with HNSCC tumors is also reflected in some clinical grades and stages. (Supplementary Table 1). In addition, based on diagnostic value analysis, the ROC curve and AUC value analysis of ITGA5 were relatively significant (Fig. 1F). Meanwhile, the nomogram of these three genes showed that ITGA5 had a greater value in the overall prognostic score than FN1 and ABL2 (Fig. 1G). In summary, ITGA5 has a relatively significant expression in HNSCC, which may be a typical risk factor for this disease.

Survival prognosis and expression of ITGA5 in HNSCC

Based on the screening results, ITGA5 was initially identified as the target gene, but to further compare the survival prognostic value of these three genes, we conducted survival prognostic analysis based on the samples of TCGA-HNSCC patients. The results showed that there were significant risk characteristics in the three survival prognostic analysis models (Overall Survival, OS; Disease Specific Survival, DSS; Progress Free Interval PFI) (HR > 1), and the high expression group of ITGA5 showed significantly lower survival (Fig. 2A-C, P < 0.05). The other two genes also showed risk characteristics (HR > 1), but they were less typical than ITGA5 (Supplementary Fig. 2A-F). Therefore, we finally choose ITGA5 as the object of exploration based on comprehensive comparison.

To verify ITGA5 expression for the HNSCC tissue, we found that ITGA5 staining in tumor tissues was more significant than that in adjacent tissues according to HNSCC-IHC (Immunohistochemical) images collected in The Human Protein Atlas (THPA) database (Due to the limitation of our objective conditions, we could not directly use human tissue for immunohistochemical detection) (Fig. 2D, E). Meanwhile, the CCLE (Cancer Cell Line Encyclopedia) database showed that the expression level of ITGA5 mRNA showed a gradient trend in 33 HNSCC cell lines. We selected three different types of squamous cell lines for validation, such as YD-8, SNU-46, and FaDu cell lines (Fig. 2F, where the red arrow is pointing). Western blot and qPCR results showed that the ITGA5 level of WSU-HN30 (Normal cell) was similar to FaDu cells, and the SNU-46 and YD-8 cells were significantly higher than normal cell (Fig. 2G, H, **P < 0.05, ***P < 0.01). In conclusion, the expression levels of ITGA5 in the three cell lines were consistent with the CCLE database, and YD-8 and FaDu were selected as validation materials for related phenotypes.

Expression of ITGA5 promote the malignant phenotype of HNSCC cell lines

When we understood the expression level of target ITGA5, the HNSCC cell lines YD-8 and FaDu were used to construct stable cell lines. The stable knockdown strains of YD-8 cells (sh#1, sh#2-ITGA5) and stable overexpression strains of FaDu cells (oe-ITGA5) were constructed by lentivirus transfection. The phenotypes of these stable cell lines were verified by Western blot and qPCR respectively, and the results showed that the knock-down of YD-8 cells (Fig. 3A, B, *P < 0.05, **P < 0.01, ***P < 0.001) and the overexpression of FaDu cells (Fig. 3C-E, **P < 0.01, ***P < 0.001) both could satisfy experimental requirements.

Based on the two types of stable cell lines constructed above, we will explore the effect of ITGA5 on the

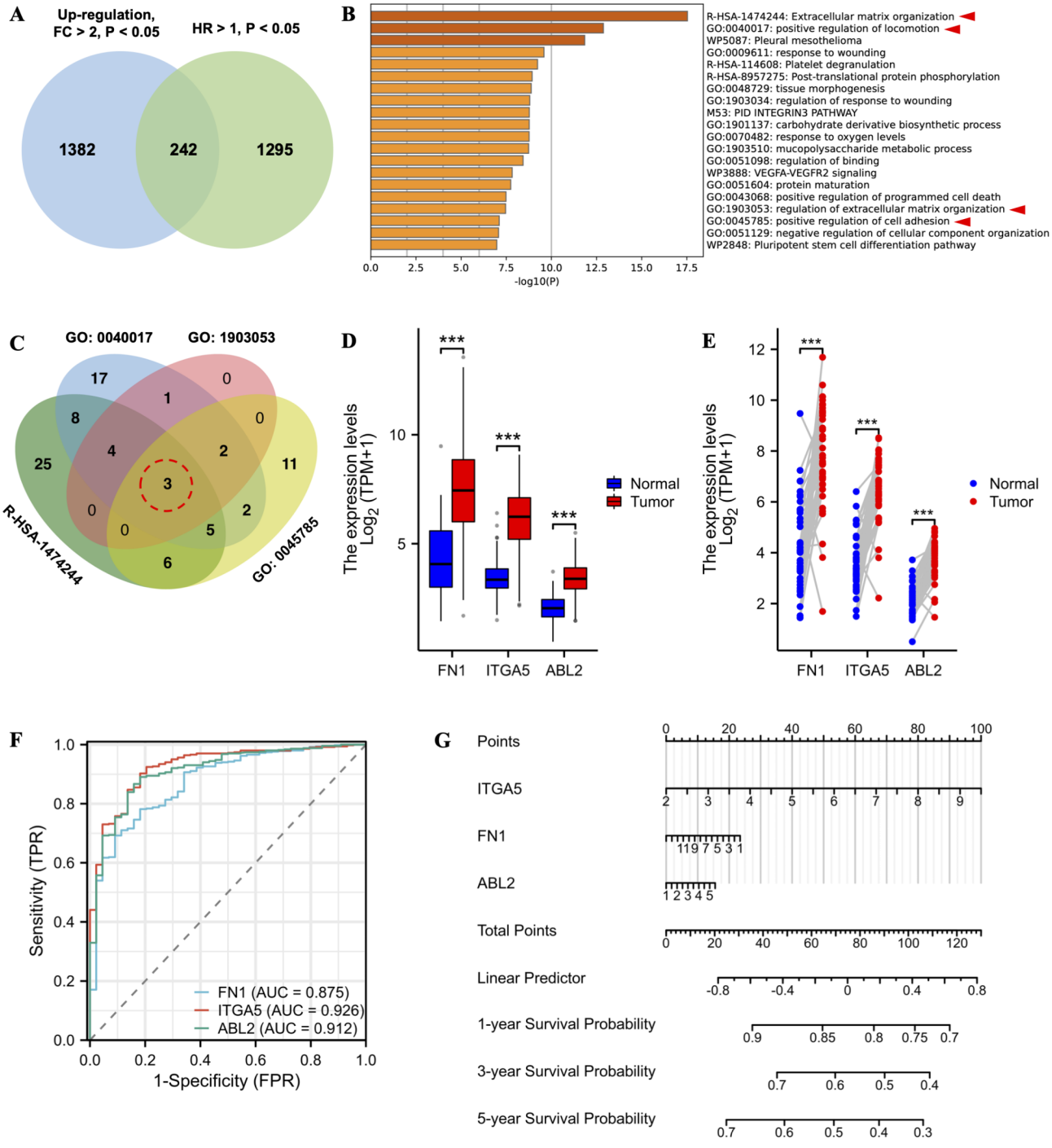

Fig. 1 Identification and screening of target genes ITGA5. **(A)** Venn diagram analysis between up-regulated genes and risk genes in TCGA-HNSCC samples; **(B)** Functional enrichment analysis of 242 genes from Fig. 1A; **(C)** Venn diagram analysis of genes from the four entries in Fig. 1B; **(D, E)** The unpaired (Tumor/Normal: 528/44) and paired (Tumor/Normal: 44/44) analysis for the three gene expressions in HNSSC, respectively; **(F)** ROC curve analysis of FN1, ITGA5 and ABL2 for HNSCC; (G) The results of nomogram analysis for FN1, ITGA5 and ABL2 in HNSCC. ***$P < 0.001$

malignant phenotype of HNSCC cell lines. Cell scratch assay showed that sh#1/2-ITGA5 significantly inhibited the migration and healing ability of YD-8 cells (Fig. 3F, H, *P < 0.05). On the contrary, oe-ITGA5 can significantly promote the phenotype of FaDu cells at 24 h and 48 h (Fig. 3G, I, *P < 0.05, **P < 0.01). In addition, Trans-well showed that sh#1/2-ITGA5 significantly inhibited the migration ability of YD-8 cells (Fig. 3J, L, **P < 0.01), and the oe-ITGA5 can significantly promote the migration of FaDu cells (Fig. 3K, M, **P < 0.01). These phenotypes

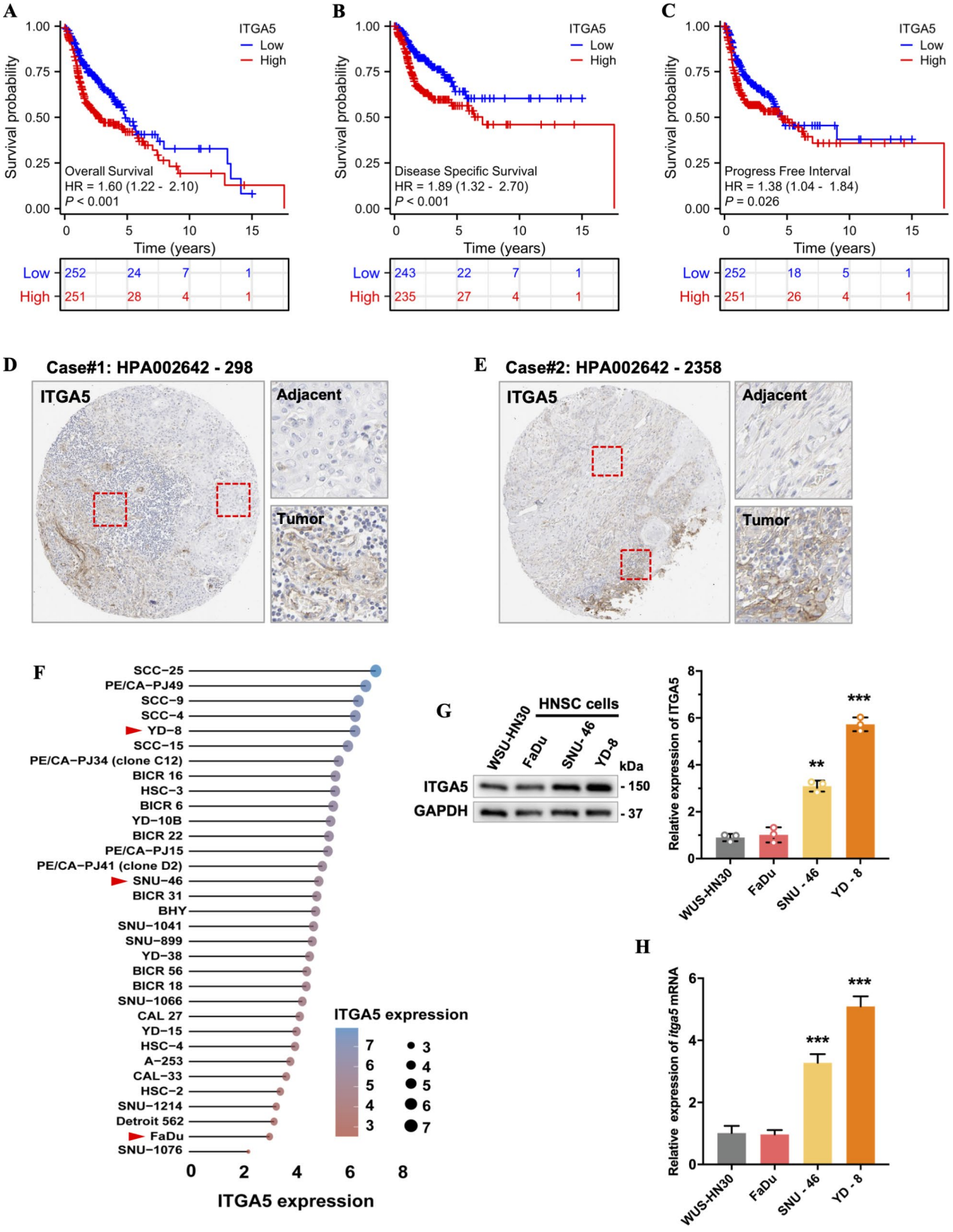

Fig. 2 The results of survival prognosis and expression of ITGA5 in HNSCC. **(A-C)** represents survival prognosis analysis of ITGA5 for OS, DSS and PFI for HNSCC, respectively; **(D, E)** represents IHC images of ITGA5 expression in HNSCC tissues from THPA database (Samples ID: HPA002642–298, 2358); **(F)** The expression levels of ITGA5 mRNA in 33 HNSCC cell lines from CCLE database; **(G, H)** represents the expression of ITGA5 in WSU-HN30, FaDu, SNU-46 and YD-8 cell lines verified by Western blot and qPCR, respectively. $^{**}P < 0.01$, $^{***}P < 0.001$

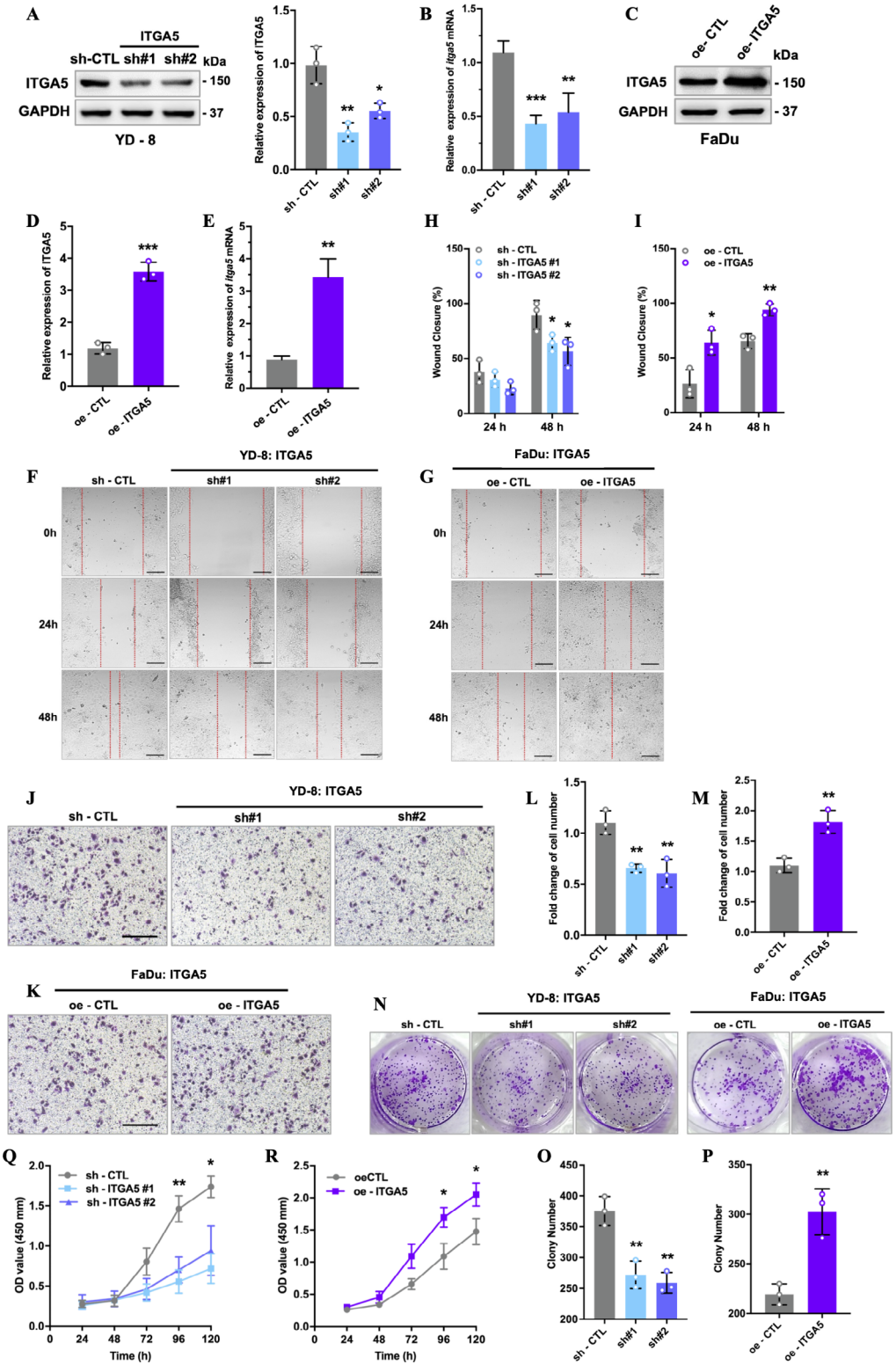

Fig. 3 ITGA5 promote the malignant phenotype of YD-8 and FaDu cell lines. **(A-E)** represents the expression of ITGA5 in sh#1/2-ITGA5 and oe-ITGA5 stable cell lines verified by Western blot and qPCR, respectively; **(F-I)** The effects of sh#1/2-ITGA5 and oe-ITGA5 on cell healing ability was verified by cell scratch assay, respectively; **(J-M)** The effects of sh#1/2-ITGA5 and oe-ITGA5 on cell migration ability were verified by Trans-well experiments, respectively; **(N-P)** The effect of sh#1/2-ITGA5 and oe-ITGA5 on cell clonal ability was verified by cell clonal formation experiments, respectively; **(Q, R)** The effects of sh#1/2-ITGA5 and oe-ITGA5 on cell growth were verified by cell proliferation experiments, respectively. *$P < 0.05$, **$P < 0.01$, ***$P < 0.001$

are consistent with the results of cell scratch experiment, which indicating that ITGA5 expression levels can affect the migration of these two HNSCC cells.

To further explore the effect of ITGA5 on cell proliferation, we verified it by cell cloning experiment. The results showed that sh#1/2-ITGA5 could significantly inhibit the clonal formation of YD-8 cells, whereas oe-ITGA5 could significantly promote the clonal formation of FaDu cells (Fig. 3N-P, $^{**}P<0.01$). Meanwhile, the proliferation curves of the two types of cell lines were measured by CCK-8 experiments (OD450). The results showed that sh#1/2-ITGA5 could significantly inhibit the proliferation of YD-8 cells, and the oe-ITGA5 could significantly promote the proliferation of FaDu cells (Fig. 3Q, R, $^{*}P<0.05$, $^{**}P<0.01$). This result is consistent with cell cloning experiment. In summary, we verified that the expression level of ITGA5 can significantly affect the malignant phenotype of tumor cells based on two HNSCC cells.

The function of ITGA5-related genes is associated to immune infiltration in HNSCC

Based on the high expression of ITGA5 can promote malignant phenotypes of HNSCC cells (e.g., cell migration and proliferation), we need to further understand the function of ITGA5 via its positive related genes. Based on TCGA-HNSCC database, we conducted enrichment analysis (KEGG and GO) of 546 genes positively related to ITGA5 (Spearman > 0.5, $P<0.05$). The results showed that the first three entries in the top 20 were the most significant (Fig. 4A, -Log10 (P-value) > 38, red arrow), which were mainly involved in the organization and formation of extracellular matrix, which may regulate cell migration activities. We performed a Venn diagram analysis from the genes of three biological processes, which showed that 26 genes were common parts (Fig. 4B). Meanwhile, the correlation between ITGA5 and HNSCC immune infiltration showed that the eosinophils and macrophages were relatively significant (Fig. 4C, $R>0.4$, $^{***}P<0.001$). Subsequently, the results of correlation analysis reflected that the marker/secretion phenotype of M2 type macrophages (M2 Φ) had the most significant (positive) correlation with 26 genes, especially TGFB1, PDGFA and PDGFB (Fig. 4D, $R>0.35$, $^{*}P<0.05$, red box). The expression difference of TGFB1, PDGFA and PDGFB in TCGA-HNSCC reflects that TGFB1 is the most significant in HNSCC (Fig. 4E, $^{***}P<0.001$). Meanwhile, these three genes showed significant risk characteristics from the survival prognosis of HNSCC (Fig. 4F-H, $HR>1$, $P<0.05$). In addition, the expression levels of TGFB1, PDGFA and PDGFB were also significantly different in tumor and adjacent tissues (Fig. 4I-K). In conclusion, ITGA5 - related genes are significantly associated with M2 macrophages in HNSCC, which also reflects that extracellular matrix and collagen formation in HNSCC cells are associated to immune infiltration of M2 macrophages.

The function of ITGA5 was verified by difference analysis of single genes

To further verify the function of ITGA5, we performed a single gene difference analysis of ITGA5. The TCGA-HNSCC samples were divided into high expression and low expression group (ITGA5, High: 252 cases /Low: 252 cases, Supplementary materials_1), and then the difference between the groups was analyzed. GO and KEEG enrichment analysis of these differential genes showed that Biological Process (BP, top 5), Cell Component (CC, top 3), and Molecular Function (MF, top 4) all exhibit extracellular matrix related functions (red arrow) (Fig. 5A). KEGG (top 4) results show extracellular matrix, adhesion, and PI3K-AKT pathway (red arrow) (Fig. 5A). To more intuitively show the relationship between various functional modules, we use EMAP plot network diagram to present the enrichment results. The results show that extracellular matrix interaction, cell adhesion and PI3K-AKT are related to the organization and dynamics of extracellular matrix (Fig. 5B). Meanwhile, this conclusion was also confirmed by GSEA enrichment analysis of these differential genes, which including extracellular matrix organization, degradation, matrix metalloproteinase activity, matrix collagen interaction, PI3K-AKT and TGFβ pathways (Fig. 5C-H, $NES>2$, $P.adj<0.001$, $FDR<0.001$). In addition, based on the background of single gene differences analysis for TGFB1, PDGFA and PDGFB, the results of GSEA enrichment analysis were consistent with ITGA5 (Supplementary Fig. 3A-C).

To further verify the function of the above enrichment pathway, we verified the phenotypes of related proteins based on ITGA5 overexpression and knockdown cell stable strains. The results showed that typical collagen I/IV and matrix metalloproteinase (MMP) 2/9 were upregulated in YD-8 and FaDu cells overexpressing ITGA5. Meanwhile, the effect was reversed in ITGA5 knockdown cells (sh#1) (Fig. 5I). The results showed that the expression level of ITGA5 in the two HNSCC cell lines showed a positive synergistic effect with collagen I/IV and MMP2/9. In addition, based on network analysis, we detected the activity of the PI3K-AKT-mTOR pathway, and the results showed that ITGA5 overexpression in the two cell lines can positively regulate the activity of this pathway (Fig. 5I). In contrast, the activity of this pathway decreased significantly under the knock-down effect of ITGA5.These results suggest that the expression of ITGA5 and its related genes in HNSCC may be involved in the regulation of extracellular matrix processes, and this conclusion can also be reflected by the expression of ITGA5-related extracellular matrix collagen and MMP in

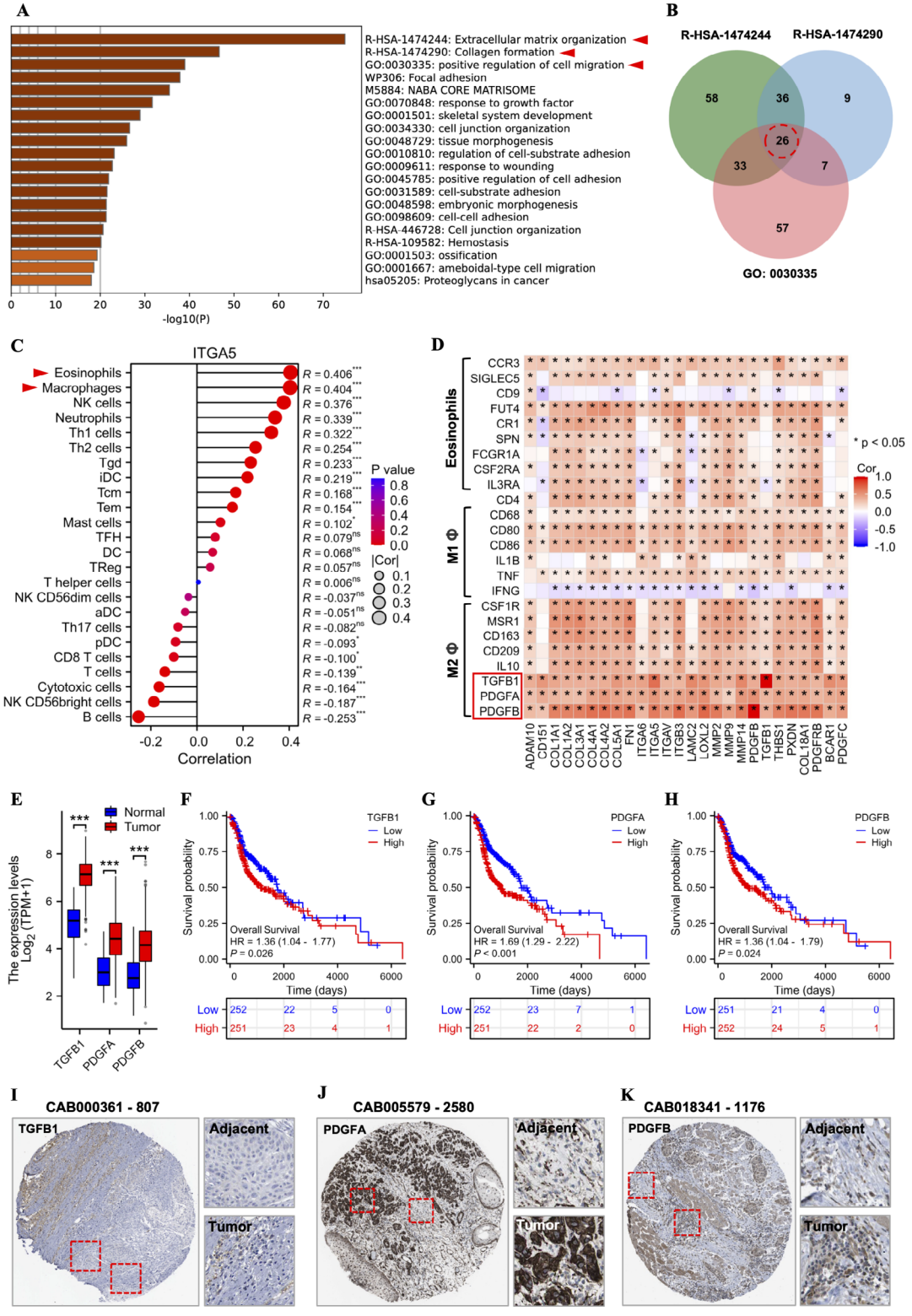

Fig. 4 The function and immune infiltration of ITGA5 related genes. **(A)** The results of functional enrichment analysis of ITGA5 and its related genes (KEGG, GO); **(B)** Venn diagram analysis of genes from the three entries in Fig. 4A; **(C)** Correlation analysis of ITGA5 with immune cell infiltration in HNSCC; **(D)** Correlation analysis of 26 genes from Fig. 4B with eosinophils, M1/M2 macrophage markers and secretion phenotypes; **(E)** Expression analysis of TGFB1, PDGFA and PDGFB in HNSCC (TCGA); **(F-H)** represents the results of OS survival prognosis analysis for TGFB1, PDGFA, and PDGFB, respectively; **(I-K)** represents the IHC image of TGFB1, PDGFA and PDGFB in HNSCC from THPA database, respectively. **P* < 0.05, ***P* < 0.01, ****P* < 0.001

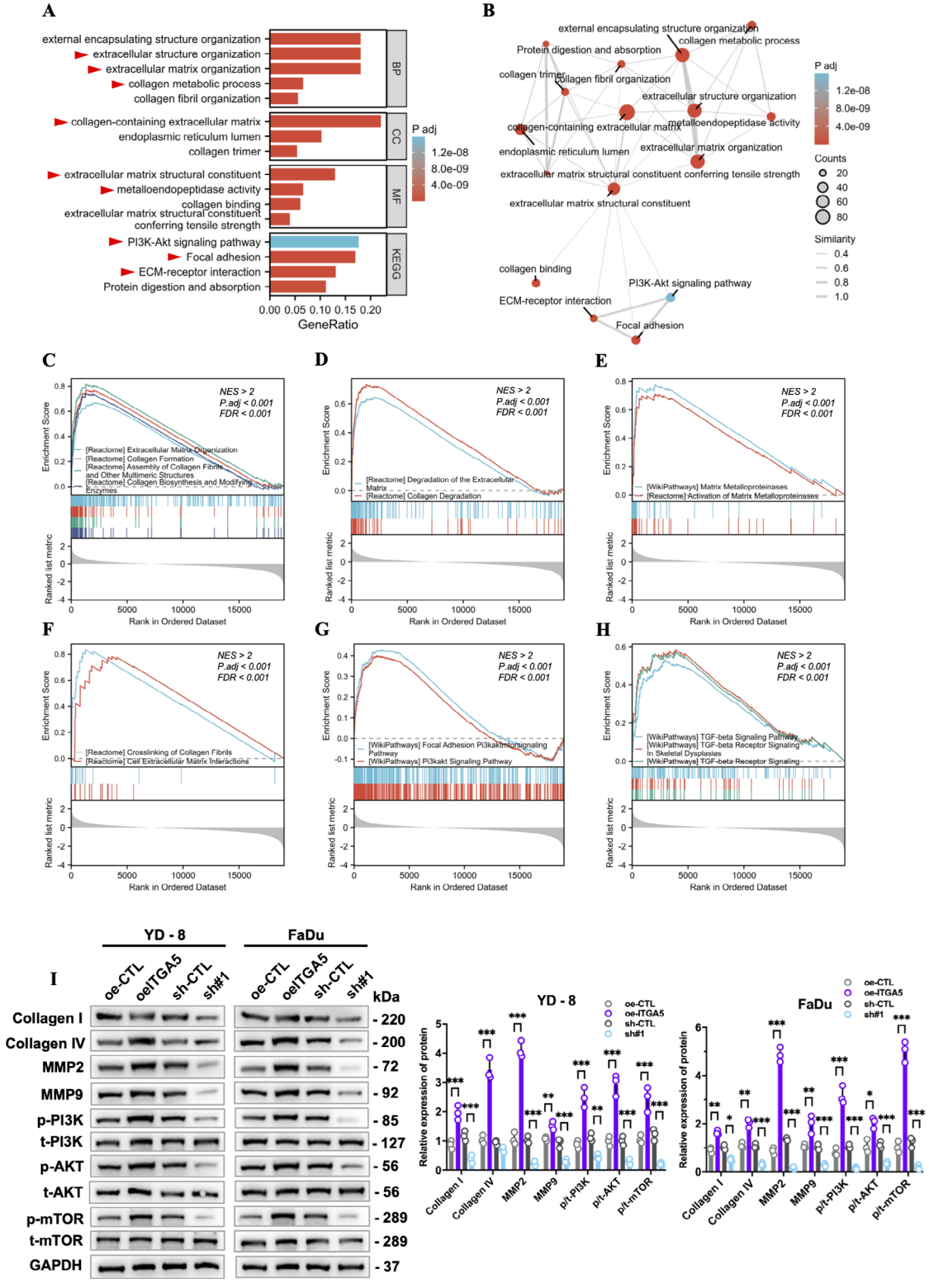

Fig. 5 Single gene difference analysis of ITGA5 for HNSCC. **(A)** The functional enrichment analysis based on results of ITGA5 single gene difference analysis; **(B)** EMAP plot network analysis based on functional enrichment analysis in Fig. 5A; **(C-H)** The results of GSEA enrichment analysis based on single gene difference analysis of ITGA5, respectively. NES > 2, *P.* adj < 0.001, FDR < 0.001. **(I)** Western blot analysis of collagen I/IV, MMP2/9, PI3K-AKT-mTOR pathway protein expression in YD-8/FaDu stable cell lines with ITGA5 overexpression and knockdown (sh#1). "p-" and "t-" indicate phosphorylated and total level, respectively

immunohistochemical results of HNSCC. (Fig. 4D, Supplementary Fig. 4A-F).

Correlation of ITGA5 with immunosuppressive phenotypes in HNSCC

It has been reported that M2 macrophages can promote the malignant progression of tumors and can induce the immunosuppressive phenotype of tumors [26–28]. Therefore, we need to further explore the correlation between ITGA5 and HNSCC immunosuppressive phenotype, we analyzed the expression of five immunosuppressive receptors and the corresponding four immune checkpoints in tumor cells. The results showed that except for CD24, all the others were significantly upregulated (Fig. 6A, C, $^{**}P<0.01$, $^{***}P<0.001$). Meanwhile, ROC curve analysis of these nine receptors or ligands showed that the AUC>0.6, which indicating that they are all valuable in diagnosing HNSCC (Fig. 6B, D). Subsequently, we investigated the correlation between ITGA5 and the expression of four immunosuppressive receptors in HNSCC. The results showed that ITGA5 was positively correlated with CD274, PDCD1LG2, CD47 and HLA-A, among which PDCD1LG2 and CD47 were the most significant (Fig. 6E-H). To further display the expression of PDCD1LG2, CD47 and corresponding immune checkpoint PDCD1, SIRPA, we presented the IHC results of HNSCC-related tissues based on the THPA database (Fig. 6I-L). In summary, ITGA5 is associated with the four immunosuppressive receptors of HNSCC.

ITGA5 is correlated with resistance of the PI3K-AKT target in HNSCC

Based on the results of differential enrichment analysis of up-regulated genes and single-gene ITGA5 in TCGA-HNSCC (Fig. 5A, B; Supplementary Fig. 1A), we found that the relevant functions of ITGA5 are involved in the PI3K-AKT pathway, which has been confirmed by some studies [29, 30]. Therefore, we need to consider the effects of ITGA5 expression for the PI3K-AKT target therapy. The correlation analysis based on Genomics of Drug Sensitivity in Cancer (GDSC, based on experimental data from tumor cells) database and TCGA-HNSCC showed that the IC50 of three PI3K inhibitors (PIK-93, ZSTK474, CAL-101) and one AKT inhibitor (GSK690693) was positively correlated with ITGA5 expression (Fig. 7A-D, $P<0.001$). These features suggest that ITGA5 expression may significantly influence resistance to PI3K-AKT target therapy.

Discussion

As a multi-system tumor type, HNSCC is mainly characterized by malignant phenotypes caused by mucosal carcinogenesis, such as high metastasis, invasiveness, immune infiltration and drug resistance [3–5]. This mucosal disease is caused by chronic infection with viruses, such as HPV and EBV [3, 31]. In addition, HNSCC caused by smoking and environmental pollution is a serious threat to people's health [3, 4]. The metastasis and immunosuppressive phenotype of HNSCC cells are the focus and difficulty for clinical treatment, and we need to combine these characteristics to explore the mechanism about the adaptive survival of tumor cells [4, 32]. For example, it has been reported that the dynamic activity of HNSCC extracellular matrix may be the basis of tumor cell metastasis [33–35], which is mainly risk factors reflected in the formation or metabolism of extracellular collagen and the activity of matrix metalloproteinases (MMPs) [35–39] (Fig. 1B, Supplementary Fig. 1A, B). Therefore, based on the clinical phenotype of HNSCC, it is necessary to seek a target or marker that can systematically reflect or predict the disease [40, 41].

In this study, ITGA5 was selected from the perspective of risk factors of HNSCC, and as a more typical gene (Fig. 1D-G), ITGA5 showed good value in the prediction and prognosis of the disease (Fig. 2). ITGA5 has been shown to be correlated with proliferation, metastasis, invasion and epithelial-mesenchymal transformation (EMT) of HNSCC cells [42–44], and some phenotypes have been validated in this study (Fig. 3). However, the value of ITGA5 in HNSCC has not been fully studied from a systematic perspective, such as the internal and external correlations or influences. Our aim is to fully explore the regulatory role of ITGA5 in HNSCC, and to analyze and verify the potential association with ITGA5 based on the metastatic and immunosuppressive phenotypes of mucosal cell carcinomas. This study shows that ITGA5 is closely associated with M2 macrophages (Fig. 4C, D), and its correlation was verified by the secretion phenotypes of TGFB1, PDGFA and PDGFB (Fig. 4D-K). This correlation is due to the dynamic processes of ITGA5 in the extracellular matrix or cell migration [45, 46]. Therefore, ITGA5 may be a biomarker for the correlation between HNSCC metastasis and immune infiltration (M2 Φ) phenotypes [10, 47]. Studies have shown that ITGA5 in gastric cancer, glioma, breast cancer and liver cancer is correlated with immune infiltration of M2 Φ, which may be involved in the regulation of tumor microenvironment and significantly affect the progression of the disease and immunosuppressive phenotype [10, 16, 28, 48, 49]. In addition, TGF-β, as an important factor affecting the HNSCC tumor microenvironment, which has become a key target for clinical treatment [50–53]. It mainly affects the proliferation of tumor cells, the dynamics and metastasis of extracellular matrix, and the generation of immunosuppressive phenotypes [53, 54]. Our study shows that the single gene difference analysis of ITGA5 and functional enrichment results include the TGFB1 related pathway, which is the first discovery in

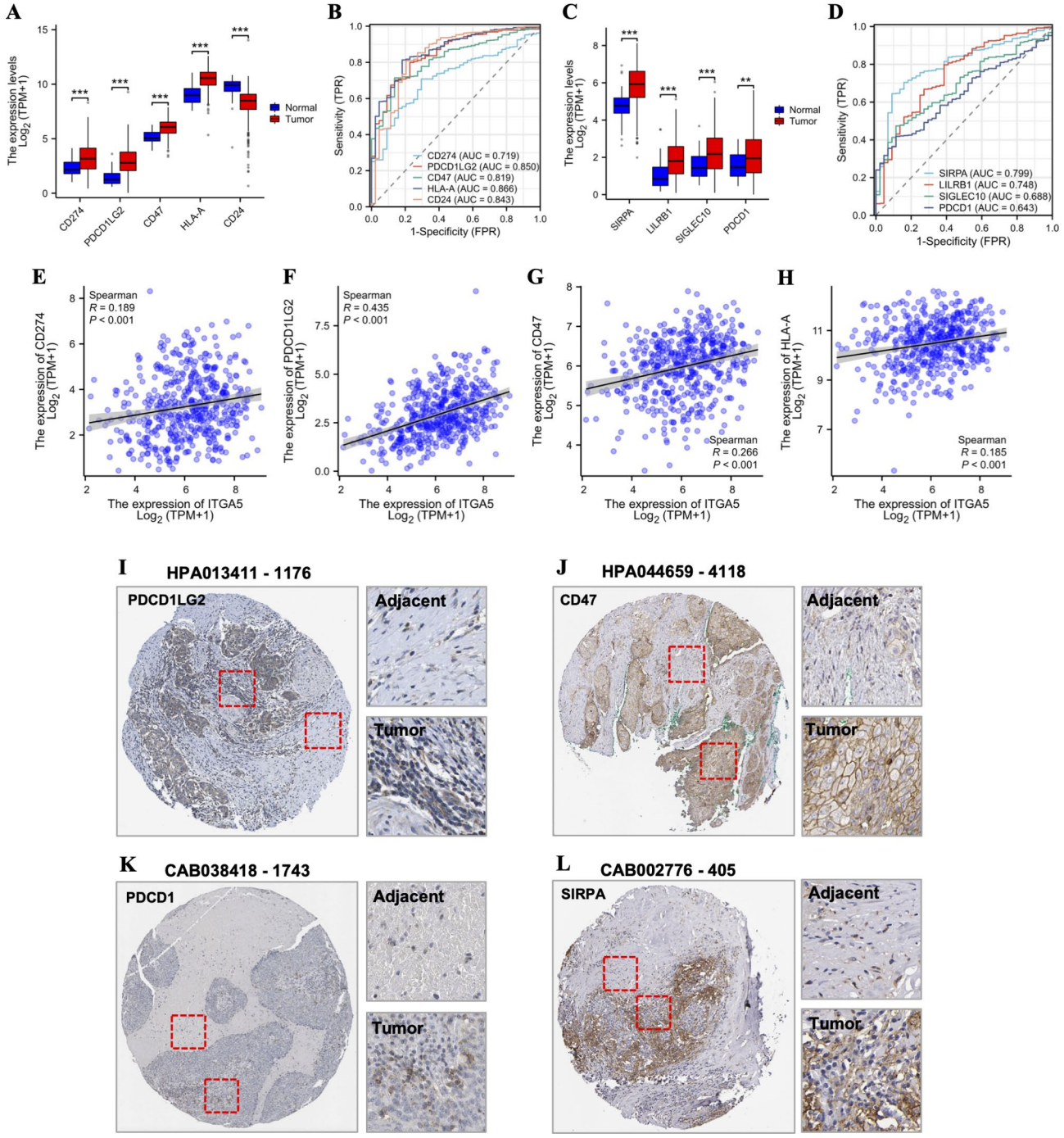

Fig. 6 Correlation of ITGA5 with immunosuppressive phenotypes in HNSCC. **(A, B)** represents the expression and ROC curve analysis of five immunosuppressive phenotypes from tumor cells, respectively; **(C, D)** represents the expression and ROC curve analysis of the four immune checkpoints from immune cells, respectively; **(E-H)** represents the scatterplot correlation analysis between ITGA5 and CD274, PDCD1LG2, CD47, HLA-A, respectively; **(I-L)** represents the IHC images of PDCD1LG2, CD47, PDCD1 and SIRPA from THPA database, respectively

this study (Fig. 5, Supplementary Fig. 3). Therefore, a systematic understanding of the external effects and associations of ITGA5 is an important basis for the prediction and prognosis of patients with HNSCC.

Based on the association between ITGA5 and M2 Φ - TGFB1, it is necessary to analyze the correlation between ITGA5 and the immunosuppressive phenotype of tumor cells [55, 56]. As expected, ITGA5 showed significant positive correlation with CD274, PDCD1LG2, CD47 and HLA-A, among which PDCD1LG2 and CD47 were the most typical (Fig. 4D). These results reflect that HNSCC cells may be regulated by extracellular matrix (ITGA5)

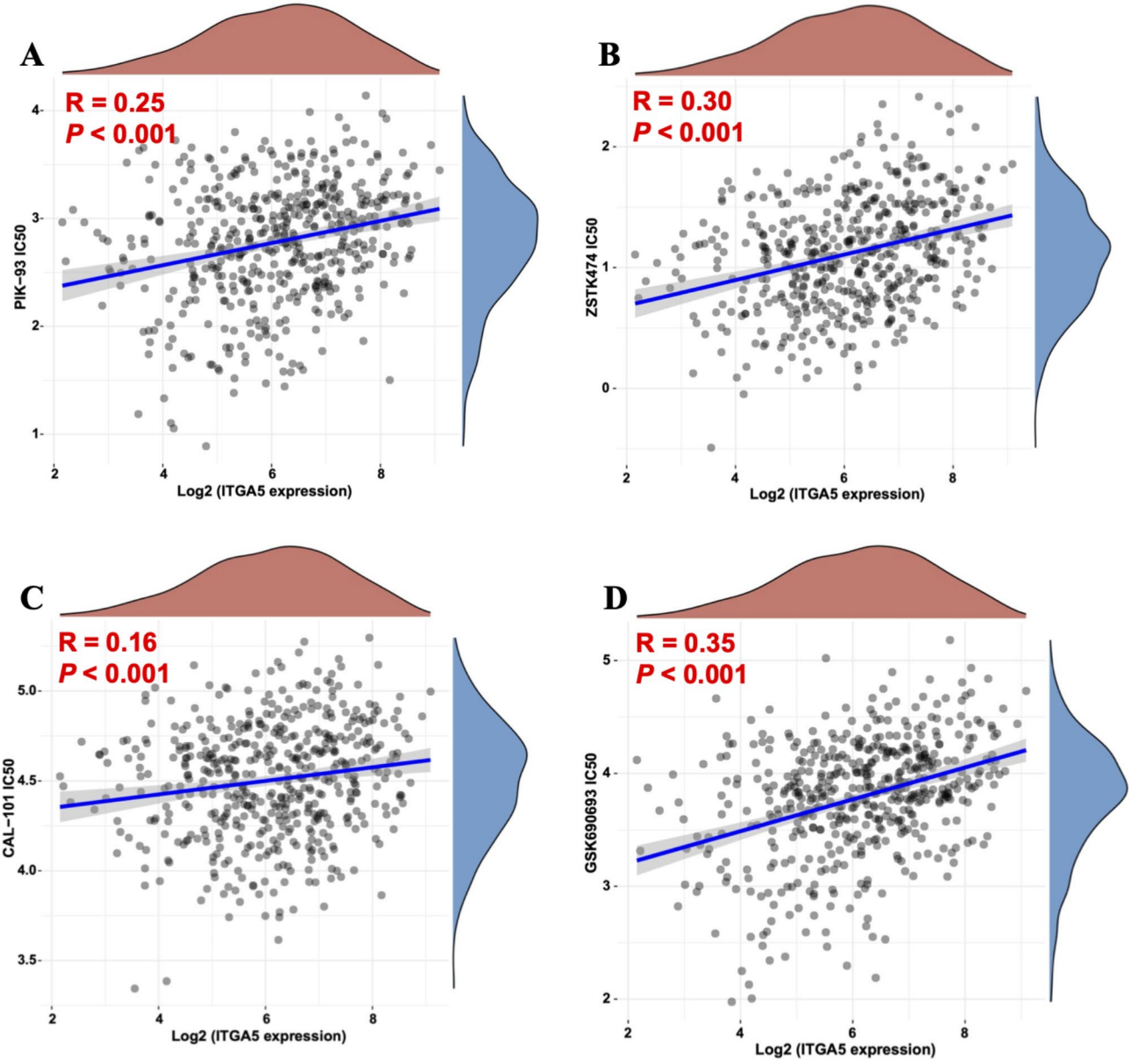

Fig. 7 Correlation analysis of ITGA5 expression and drug sensitivity (IC50) for PI3K-AKT in HNSCC. **(A-D)** represents correlation analysis between ITGA5 expression and IC50 of inhibitors PI-K93, ZSTK474, CAL-101 and GSK690693, respectively

and TGF-β from the tumor microenvironment under the influence mechanism of ITGA5/TGFB1, and thus produce an immunosuppressive phenotype [10, 16, 57]. Studies have shown that extracellular matrix and TGF-β in the tumor microenvironment can affect the immunosuppressive phenotype and immune checkpoint of tumor cells [58], and these effects may become an important perspective for HNSCC treatment [57, 59]. Therefore, combined with the results in this study, it is suggested that the intrinsic and extrinsic functions involved in ITGA5 may benefit to the adaptive survival and progression of HNSCC (Figs. 2A-C and 4F-H). In addition, ITGA5 can affect tumor progression and chemotherapy resistance via the PI3K-AKT pathway, which has been confirmed by studies [30, 60–62]. Based on this, we identified a positive correlation between ITGA5 and the resistance of the targeting PI3K-AKT, which reflects that the expression of ITGA5 may affect the efficacy of chemotherapy for targeting PI3K-AKT (Fig. 7A-D).

In summary, although we explored the systematic correlations and influence of ITGA5 in HNSCC, and we discussed the correlation between tumor cell metastasis, immune infiltration and immunosuppressive phenotype. However, further experiments are needed to confirm these conclusions, especially the external effects of ITGA5 on the tumor microenvironment. Based on the

systematic analysis and exploration of this study, compared with previous studies, the characteristics of multi-phenotype interlinkages are highlighted, which reflects that ITGA5 may be a potential marker or therapeutic target.

Supplementary Information

The online version contains supplementary material available at https://doi.org/10.1186/s13000-024-01559-1.

Supplementary Material 1

Supplementary Material 2

Supplementary Material 3

Supplementary Material 4: Fig. 1. The bubble map based on functional enrichment analysis of TCGA-HNSCC differential genes (Tumor vs. adjacent). (A, B) represents KEGG and GO functional enrichment analysis of up-regulated genes in HNSCC, respectively; (C, D) represents KEGG and GO functional enrichment analysis of down-regulated genes in HNSCC, respectively.

Supplementary Material 5: Fig. 2. (A-C) represents survival prognosis analysis of OS, DSS and FPI for FN1 in TCGA-HNSCC, respectively; (D-F) represents survival prognosis analysis of OS, DSS and FPI for ABL2 in TCGA-HNSCC, respectively.

Supplementary Material 6: Fig. 3. (A-C) represents GSEA functional enrichment analysis based on single gene difference analysis of TGFB1, PDGFA and PDGFB in TCGA-HNSCC, respectively.

Supplementary Material 7: Fig. 4. (A-F) represents the IHC images of COL1A1, COL3A1, COL4A1, COL5A1, MMP2 and MMP9 in HNSCC from THPA database, respectively.

Acknowledgements
We are especially grateful for the Sichuan Cancer Hospital, Department of Head and Neck Surgery; People's Hospital of Deyang City, Department of Otolaryngology Head and Neck surgery.

Author contributions
Study concept and design: JL and MZ; Acquisition of data: JL, YW and XC; Analysis and interpretation of data: JL and YW; Statistical analysis: XC; Drafting of the manuscript: JL and XC; Manuscript check: XC, XC and MZ; Critical revision and final approval of the manuscript: MZ. All authors contributed to the article and approved the submitted version.

Funding
This study was not supported by any funding.

Data availability
No datasets were generated or analysed during the current study.

Declarations

Consent for publication
All personal data and samples involved in this study have been obtained with their knowledge and permission for publication.

Competing interests
The authors declare no competing interests.

Ethics Statement
The studies involving data and platform were reviewed and approved by The Institutional Research Ethics Committee of Sichuan Cancer Hospital.

Received: 10 July 2024 / Accepted: 28 September 2024
Published online: 07 October 2024

References

1. Sung H, Ferlay J, Siegel RL, Laversanne M, Soerjomataram I, Jemal A, Bray F. Global Cancer statistics 2020: GLOBOCAN estimates of incidence and Mortality Worldwide for 36 cancers in 185 countries. CA Cancer J Clin. 2021;71:209–49.
2. Ferlay J, Colombet M, Soerjomataram I, Mathers C, Parkin DM, Pineros M, Znaor A, Bray F. Estimating the global cancer incidence and mortality in 2018: GLOBOCAN sources and methods. Int J Cancer. 2019;144:1941–53.
3. Johnson DE, Burtness B, Leemans CR, Lui VWY, Bauman JE, Grandis JR. Head and neck squamous cell carcinoma. Nat Rev Dis Primers. 2020;6:92.
4. Ruffin AT, Li H, Vujanovic L, Zandberg DP, Ferris RL, Bruno TC. Improving head and neck cancer therapies by immunomodulation of the tumour microenvironment. Nat Rev Cancer. 2023;23:173–88.
5. Solomon B, Young RJ, Rischin D. Head and neck squamous cell carcinoma: Genomics and emerging biomarkers for immunomodulatory cancer treatments. Semin Cancer Biol. 2018;52:228–40.
6. Mei Z, Huang J, Qiao B, Lam AK. Immune checkpoint pathways in immunotherapy for head and neck squamous cell carcinoma. Int J Oral Sci. 2020;12:16.
7. Oliva M, Spreafico A, Taberna M, Alemany L, Coburn B, Mesia R, Siu LL. Immune biomarkers of response to immune-checkpoint inhibitors in head and neck squamous cell carcinoma. Ann Oncol. 2019;30:57–67.
8. Elmusrati A, Wang J, Wang CY. Tumor microenvironment and immune evasion in head and neck squamous cell carcinoma. Int J Oral Sci. 2021;13:24.
9. Yilmaz E, Ismaila N, Bauman JE, Dabney R, Gan G, Jordan R, Kaufman M, Kirtane K, McBride SM, Old MO, et al. Immunotherapy and Biomarker Testing in Recurrent and Metastatic Head and Neck cancers: ASCO Guideline. J Clin Oncol. 2023;41:1132–46.
10. Zhu H, Wang G, Zhu H, Xu A. ITGA5 is a prognostic biomarker and correlated with immune infiltration in gastrointestinal tumors. BMC Cancer. 2021;21:269.
11. Wang X, Che X, Yu Y, Cheng Y, Bai M, Yang Z, Guo Q, Xie X, Li D, Guo M, et al. Hypoxia-autophagy axis induces VEGFA by peritoneal mesothelial cells to promote gastric cancer peritoneal metastasis through an integrin alpha5-fibronectin pathway. J Exp Clin Cancer Res. 2020;39:221.
12. Kuninty PR, Bansal R, De Geus SWL, Mardhian DF, Schnittert J, van Baarlen J, Storm G, Bijlsma MF, van Laarhoven HW, Metselaar JM, et al. ITGA5 inhibition in pancreatic stellate cells attenuates desmoplasia and potentiates efficacy of chemotherapy in pancreatic cancer. Sci Adv. 2019;5:eaax2770.
13. Xiao Y, Li Y, Tao H, Humphries B, Li A, Jiang Y, Yang C, Luo R, Wang Z. Integrin alpha5 down-regulation by miR-205 suppresses triple negative breast cancer stemness and metastasis by inhibiting the Src/Vav2/Rac1 pathway. Cancer Lett. 2018;433:199–209.
14. Li XQ, Zhang R, Lu H, Yue XM, Huang YF. Extracellular vesicle-packaged CDH11 and ITGA5 induce the Premetastatic Niche for Bone colonization of breast Cancer cells. Cancer Res. 2022;82:1560–74.
15. Pavlakis E, Neumann M, Merle N, Wieboldt R, Wanzel M, Ponath V, Pogge von Strandmann E, Elmshauser S, Stiewe T. Mutant p53-ENTPD5 control of the calnexin/calreticulin cycle: a druggable target for inhibiting integrin-alpha5-driven metastasis. J Exp Clin Cancer Res. 2023;42:203.
16. Li S, Zhang N, Liu S, Zhang H, Liu J, Qi Y, Zhang Q, Li X. ITGA5 is a Novel Oncogenic Biomarker and correlates with Tumor Immune Microenvironment in Gliomas. Front Oncol. 2022;12:844144.
17. Zou B, Wang D, Xu K, Yuan DY, Meng Z, Zhang B. Integrin alpha-5 as a potential biomarker of head and neck squamous cell carcinoma. Oncol Lett. 2019;18:4048–55.
18. Zhou C, Shen Y, Wei Z, Shen Z, Tang M, Shen Y, Deng H. ITGA5 is an independent prognostic biomarker and potential therapeutic target for laryngeal squamous cell carcinoma. J Clin Lab Anal. 2022;36:e24228.
19. Feng C, Jin X, Han Y, Guo R, Zou J, Li Y, Wang Y. Expression and prognostic analyses of ITGA3, ITGA5, and ITGA6 in Head and Neck squamous cell carcinoma. Med Sci Monit. 2020;26:e926800.
20. Zhou Y, Zhou B, Pache L, Chang M, Khodabakhshi AH, Tanaseichuk O, Benner C, Chanda SK. Metascape provides a biologist-oriented resource for the analysis of systems-level datasets. Nat Commun. 2019;10:1523.
21. Subramanian A, Tamayo P, Mootha VK, Mukherjee S, Ebert BL, Gillette MA, Paulovich A, Pomeroy SL, Golub TR, Lander ES, Mesirov JP. Gene set enrichment analysis: a knowledge-based approach for interpreting genome-wide expression profiles. Proc Natl Acad Sci U S A. 2005;102:15545–50.
22. Liu J, Lichtenberg T, Hoadley KA, Poisson LM, Lazar AJ, Cherniack AD, Kovatich AJ, Benz CC, Levine DA, Lee AV, et al. An Integrated TCGA Pan-cancer Clinical Data Resource to Drive High-Quality Survival Outcome Analytics. Cell. 2018;173:400–e416411.

23. Hanzelmann S, Castelo R, Guinney J. GSVA: gene set variation analysis for microarray and RNA-seq data. BMC Bioinformatics. 2013;14:7.
24. Lu X, Jiang L, Zhang L, Zhu Y, Hu W, Wang J, Ruan X, Xu Z, Meng X, Gao J, et al. Immune signature-based subtypes of cervical squamous cell Carcinoma tightly Associated with Human Papillomavirus Type 16 expression, molecular features, and clinical outcome. Neoplasia. 2019;21:591–601.
25. Geeleher P, Cox NJ, Huang RS. Clinical drug response can be predicted using baseline gene expression levels and in vitro drug sensitivity in cell lines. Genome Biol. 2014;15:R47.
26. Qiu Y, Chen T, Hu R, Zhu R, Li C, Ruan Y, Xie X, Li Y. Next frontier in tumor immunotherapy: macrophage-mediated immune evasion. Biomark Res. 2021;9:72.
27. Mantovani A, Allavena P, Marchesi F, Garlanda C. Macrophages as tools and targets in cancer therapy. Nat Rev Drug Discov. 2022;21:799–820.
28. Wei Z, Zhang X, Yong T, Bie N, Zhan G, Li X, Liang Q, Li J, Yu J, Huang G, et al. Boosting anti-PD-1 therapy with metformin-loaded macrophage-derived microparticles. Nat Commun. 2021;12:440.
29. Hu Q, Tian T, Leng Y, Tang Y, Chen S, Lv Y, Liang J, Liu Y, Liu T, Shen L, Dong X. The O-glycosylating enzyme GALNT2 acts as an oncogenic driver in non-small cell lung cancer. Cell Mol Biol Lett. 2022;27:71.
30. Zhang X, Chen F, Huang P, Wang X, Zhou K, Zhou C, Yu L, Peng Y, Fan J, Zhou J, et al. Exosome-depleted MiR-148a-3p derived from hepatic stellate cells promotes Tumor Progression via ITGA5/PI3K/Akt Axis in Hepatocellular Carcinoma. Int J Biol Sci. 2022;18:2249–60.
31. Leemans CR, Snijders PJF, Brakenhoff RH. The molecular landscape of head and neck cancer. Nat Rev Cancer. 2018;18:269–82.
32. Cramer JD, Burtness B, Le QT, Ferris RL. The changing therapeutic landscape of head and neck cancer. Nat Rev Clin Oncol. 2019;16:669–83.
33. Di Martino JS, Nobre AR, Mondal C, Taha I, Farias EF, Fertig EJ, Naba A, Aguirre-Ghiso JA, Bravo-Cordero JJ. A tumor-derived type III collagen-rich ECM niche regulates tumor cell dormancy. Nat Cancer. 2022;3:90–107.
34. Saint A, Van Obberghen-Schilling E. The role of the tumor matrix environment in progression of head and neck cancer. Curr Opin Oncol. 2021;33:168–74.
35. Raudenska M, Balvan J, Hanelova K, Bugajova M, Masarik M. Cancer-associated fibroblasts: mediators of head and neck tumor microenvironment remodeling. Biochim Biophys Acta Rev Cancer. 2023;1878:188940.
36. Arosarena OA, Barr EW, Thorpe R, Yankey H, Tarr JT, Safadi FF. Osteoactivin regulates head and neck squamous cell carcinoma invasion by modulating matrix metalloproteases. J Cell Physiol. 2018;233:409–21.
37. Celentano A, Yap T, Paolini R, Yiannis C, Mirams M, Koo K, McCullough M, Cirillo N. Inhibition of matrix metalloproteinase-2 modulates malignant behaviour of oral squamous cell carcinoma cells. J Oral Pathol Med. 2021;50:323–32.
38. Wang D, Pei P, Shea FF, Bissonnette C, Nieto K, Din C, Liu Y, Schwendeman SP, Lin YX, Spinney R, Mallery SR. Fenretinide combines perturbation of signaling kinases, cell-extracellular matrix interactions and matrix metalloproteinase activation to inhibit invasion in oral squamous cell carcinoma cells. Carcinogenesis. 2022;43:851–64.
39. Rosenthal EL, Zhang W, Talbert M, Raisch KP, Peters GE. Extracellular matrix metalloprotease inducer-expressing head and neck squamous cell carcinoma cells promote fibroblast-mediated type I collagen degradation in vitro. Mol Cancer Res. 2005;3:195–202.
40. Liu M, Huang L, Liu Y, Yang S, Rao Y, Chen X, Nie M, Liu X. Identification of the MMP family as therapeutic targets and prognostic biomarkers in the microenvironment of head and neck squamous cell carcinoma. J Transl Med. 2023;21:208.
41. Thangaraj SV, Shyamsundar V, Krishnamurthy A, Ramshankar V. Deregulation of extracellular matrix modeling with molecular prognostic markers revealed by transcriptome sequencing and validations in oral Tongue squamous cell carcinoma. Sci Rep. 2021;11:250.
42. Wang R, Gao Y, Zhang H. ACTN1 interacts with ITGA5 to promote cell proliferation, invasion and epithelial-mesenchymal transformation in head and neck squamous cell carcinoma. Iran J Basic Med Sci. 2023;26:200–7.
43. Li D, Sun A, Zhang L, Ding Z, Yi F, Yang X, Wang Z, Chen X, Liu W, Liu S, et al, et al. Elevated ITGA5 facilitates hyperactivated mTORC1-mediated progression of laryngeal squamous cell carcinoma via upregulation of EFNB2. Theranostics. 2022;12:7431–49.
44. Wang X, Huang J, You R, Hou D, Liu J, Wu L, Yao M, Yang F, Huang H. Downregulation of ITGA5 inhibits lymphangiogenesis and cell migration and invasion in male laryngeal squamous cell carcinoma. Protoplasma. 2023;260:1569–80.
45. Xu D, Li T, Wang R, Mu R. Expression and Pathogenic Analysis of Integrin Family genes in systemic sclerosis. Front Med (Lausanne). 2021;8:674523.
46. Li YY, Zhou CX, Gao Y. Interaction between oral squamous cell carcinoma cells and fibroblasts through TGF-beta1 mediated by podoplanin. Exp Cell Res. 2018;369:43–53.
47. Tao ZY, Yang WF, Zhu WY, Wang LL, Li KY, Guan XY, Su YX. A neural-related gene risk score for head and neck squamous cell carcinoma. Oral Dis 2022.
48. Liu S, Song A, Wu Y, Yao S, Wang M, Niu T, Gao C, Li Z, Zhou X, Huo Z, et al. Analysis of genomics and immune infiltration patterns of epithelial-mesenchymal transition related to metastatic breast cancer to bone. Transl Oncol. 2021;14:100993.
49. Hu B, Shen X, Qin W, Zhang L, Zou T, Dong Q, Qin LX. A prognostic Nomogram for Hepatocellular Carcinoma based on Wound Healing and Immune checkpoint genes. J Clin Transl Hepatol. 2022;10:891–900.
50. Pang X, Tang YL, Liang XH. Transforming growth factor-beta signaling in head and neck squamous cell carcinoma: insights into cellular responses. Oncol Lett. 2018;16:4799–806.
51. Maldonado LAG, Nascimento CR, Rodrigues Fernandes NA, Silva ALP, D'Silva NJ, Rossa C Jr. Influence of tumor cell-derived TGF-beta on macrophage phenotype and macrophage-mediated tumor cell invasion. Int J Biochem Cell Biol. 2022;153:106330.
52. Jank BJ, Schnoell J, Kladnik K, Sparr C, Haas M, Gurnhofer E, Lein AL, Brunner M, Kenner L, Kadletz-Wanke L, Heiduschka G. Targeting TGF beta receptor 1 in head and neck squamous cell carcinoma. Oral Dis 2023.
53. Taniguchi S, Elhance A, Van Duzer A, Kumar S, Leitenberger JJ, Oshimori N. Tumor-initiating cells establish an IL-33-TGF-beta niche signaling loop to promote cancer progression. Science 2020, 369.
54. Peng D, Fu M, Wang M, Wei Y, Wei X. Targeting TGF-beta signal transduction for fibrosis and cancer therapy. Mol Cancer. 2022;21:104.
55. Qi C, Lei L, Hu J, Ou S. Establishment and validation of a novel integrin-based prognostic gene signature that sub-classifies gliomas and effectively predicts immunosuppressive microenvironment. Cell Cycle. 2023;22:1259–83.
56. Chen J, Ji T, Wu D, Jiang S, Zhao J, Lin H, Cai X. Human mesenchymal stem cells promote tumor growth via MAPK pathway and metastasis by epithelial mesenchymal transition and integrin alpha5 in hepatocellular carcinoma. Cell Death Dis. 2019;10:425.
57. Redman JM, Friedman J, Robbins Y, Sievers C, Yang X, Lassoued W, Sinkoe A, Papanicolau-Sengos A, Lee CC, Marte JL et al. Enhanced neoepitope-specific immunity following neoadjuvant PD-L1 and TGF-beta blockade in HPV-unrelated head and neck cancer. J Clin Invest 2022, 132.
58. Jiao S, Subudhi SK, Aparicio A, Ge Z, Guan B, Miura Y, Sharma P. Differences in Tumor Microenvironment Dictate T Helper Lineage Polarization and response to Immune Checkpoint Therapy. Cell. 2019;179:1177–e11901113.
59. Zhang P, Zhang Y, Wang L, Lou W. Tumor-regulated macrophage type 2 differentiation promotes immunosuppression in laryngeal squamous cell carcinoma. Life Sci. 2021;267:118798.
60. Xu F, Zhou F. Inhibition of microRNA-92a ameliorates lipopolysaccharide-induced endothelial barrier dysfunction by targeting ITGA5 through the PI3K/Akt signaling pathway in human pulmonary microvascular endothelial cells. Int Immunopharmacol. 2020;78:106060.
61. Saatci O, Kaymak A, Raza U, Ersan PG, Akbulut O, Banister CE, Sikirzhytski V, Tokat UM, Aykut G, Ansari SA, et al. Targeting lysyl oxidase (LOX) overcomes chemotherapy resistance in triple negative breast cancer. Nat Commun. 2020;11:2416.
62. Assidicky R, Tokat UM, Tarman IO, Saatci O, Ersan PG, Raza U, Ogul H, Riazalhosseini Y, Can T, Sahin O. Targeting HIF1-alpha/miR-326/ITGA5 axis potentiates chemotherapy response in triple-negative breast cancer. Breast Cancer Res Treat. 2022;193:331–48.

Publisher's note